Effect of Mixing on Product Quality in Semibatch Stirred Tank Reactors

Iris L. M. Verschuren, Johan G. Wijers, and Jos T. F. Keurentjes
Dept. of Chemical Engineering and Chemistry, Process Development Group, Eindhoven University of Technology, 5600 MB Eindhoven, The Netherlands

Semibatch stirred tank reactors with a turbulent flow field are used frequently in the chemical process industry to accomplish mixing tasks. Mixing in a turbulent flow consists of several processes. Descriptions for these processes from literature are used to construct a model to calculate the selectivity of a mixing-sensitive reaction in a semibatch stirred tank reactor. The model is validated by determining the effects of various process parameters on the selectivity of the third Bourne reaction. Calculation of the selectivity requires information on the hydrodynamic parameters of the stirred vessel studied. The essential detailed description of these hydrodynamic parameters to obtain a good agreement between measured and calculated selectivities was determined. The model proved to be successful in predicting the product distribution of a competitive reaction, making it useful for the design and scale-up of stirred-tank reactors.

Introduction

Before a chemical reaction can occur between two or more reactants, the reactants have to be mixed on a molecular scale. When reaction is slow in comparison to the mixing process, the solution will be homogeneously mixed before reaction takes place and the product distribution will only depend on the chemical kinetics. However, when reaction is fast relative to the mixing rate, the mixing rate will also determine the yield and selectivity of the process. Examples of mixing sensitive reactions are monoacylation of symmetrical diamines (Jacobson et al., 1987), precipitation reactions (Franke and Mersmann, 1995) and fermentation processes (Larsson et al., 1992).

Because mixing has a large influence on the product quality of a mixing sensitive reaction, a model for the mixing of reacting flows is a helpful tool in the design of a chemical reactor. In principle, the mixing of fluids is completely described by the partial differential equations describing the momentum, mass, and species balances. However, turbulent flows contain a wide range of time and length scales and, therefore, even with the nowadays-available computational resources, the complete exact solution of these differential equations is not possible. Therefore, simplified, but tractable, models are proposed in the literature to describe the mixing in turbulent flows (see Fox, 1996, for a review). The applicability of these models depends on the type of flow and chemical reactions under consideration. Stirred-tank reactors with a turbulent flow field are commonly used in chemical and biochemical industries to accomplish mixing tasks. In this article turbulent mixing of dilute solutions of reactants in a semi-batch stirred tank reactor with a feed stream is considered for fast chemical reactions.

A fast reaction in a stirred-tank reactor takes place in a small portion of the whole vessel (Baldyga and Bourne, 1992) and the reaction zone becomes more localized when a stirred-tank reactor is scaled up with a constant power input per unit volume (Bourne and Dell'ava, 1987). For a localized reaction zone, the following processes are used to describe the mixing of fluids in a turbulent flow (Ranade and Bourne, 1991):

(1) Convection of the reaction zone through the vessel by the average velocity.

(2) Spatial evolution of the reaction zone due to turbulent dispersion by large-scale turbulent motions.

(3) Mixing of reactants in the reaction zone on a molecular scale inside small-scale turbulent motions by engulfment, deformation, and diffusion.

Models for these mixing processes are described in the literature (Baldyga and Bourne, 1984, 1989; David and Viller-

Correspondence concerning this article should be addressed to I. L. M. Verschuren.

maux, 1987). In this work a combination of these descriptions will be used to obtain a model for the calculation of the selectivity of a mixing-sensitive reaction set in a semi-batch stirred tank reactor with a feedstream.

The processes of mixing described above are determined by hydrodynamic parameters. Therefore, application of the model requires information on these hydrodynamic parameters inside the stirred vessel. The reactor type used in this study is a cylindrical vessel equipped with a Rushton turbine stirrer and four baffles. The hydrodynamic parameters for this reactor type have been determined extensively by laser doppler velocimetry experiments, as described in previous articles (Kajbic, 1995; Kusters, 1991; Schoenmakers, 1998). However, for many industrial processes these parameters are not known in great detail. Therefore, in this work it is also investigated in how much detail these hydrodynamic parameters have to be known to predict the selectivity of a mixing sensitive reaction set.

To validate the model, the selectivity of a mixing sensitive reaction set is determined experimentally for a broad range of process and design variables.

Mixing Model

Lagrangian models for the mixing processes in a turbulent flow are used to describe the mixing of the fluid elements in a stirred-tank reactor. The engulfment, deformation, and diffusion (EDD) model describes micromixing by diffusion within shrinking laminated structures formed by engulfment (Baldyga and Bourne, 1984). Baldyga and Bourne (1989a) have shown that for systems having a Schmidt number less than 4,000, engulfment is the rate-determining step of the micromixing process and the EDD-model is simplified to the engulfment model (E-model). The growth of the micromixed volume according to the E-model is

$$\frac{dV_{mi}}{dt} = EV_{mi} \tag{1}$$

$$E = 0.058\sqrt{\frac{\epsilon}{\nu}} \tag{2}$$

with V_{mi} the volume mixed on a molecular scale, E the engulfment rate, ϵ the energy dissipation rate, and ν the kinematic viscosity.

Mixing of micromixed fluid with micromixed fluid will not lead to growth of the total micromixed volume. The probability of this so-called self-engulfment depends on the volume fraction of micromixed fluid inside the spreaded feedstream. The growth of the micromixed volume taking into account possible self-engulfment (Baldyga and Bourne, 1989b) is

$$\frac{dV_{mi}}{dt} = EV_{mi}(1 - V_{mi}/V_{td}) \tag{3}$$

where V_{td} is the volume of the dispersed feedstream.

The spreading of the feedstream is characterized by a turbulent dispersion coefficient (D_t) (Nagata, 1975). David and Villermaux (1987) have used this turbulent dispersion coefficient to describe the growth of the linear dimension (L) of a cloud containing an injected scalar

$$\frac{dL^2}{dt} = D_t \quad \text{or} \quad \frac{dV_{td}}{dt} = \frac{3}{2}D_t V_{td}^{1/3} \tag{4}$$

in which the volume of the cloud is assumed to be equal to L^3 for the sake of simplicity.

As noticed by Baldyga and Pohorecki (1995), in a continuous feedstream the concentration gradients in radial direction are much larger than in the direction of the flow. Therefore, only radial dispersion is assumed and the growth of the volume of a slice, with diameter L and thickness δ, is given by (Baldyga and Pohorecki, 1995)

$$\frac{dV_{td}}{dt} = \frac{\pi}{4}\delta\frac{dL^2}{dt} = \frac{\pi}{4}\delta D_t = \frac{V_{td}}{L^2}D_t \tag{5}$$

In this study the mixing of a continuous feedstream in a stirred vessel is investigated. Therefore, Eq. 5 will probably be more appropriate for our model than Eq. 4. The turbulent dispersion coefficient in Eq. 5, used to describe the growth of V_{td}, is determined by hydrodynamic parameters. The growth of the diameter of a scalar cloud (L), with a diameter smaller or in the order of the velocity length scale (L_v), follows a Richardson Law (Lesieur, 1990)

$$\frac{1}{2}\frac{dL^2}{dt} = C\epsilon^{1/3}L^{4/3} \tag{6}$$

When the scalar cloud diameter is larger than the velocity length scale, the growth of the diameter is described by (Lesieur, 1990)

$$\frac{1}{2}\frac{dL^2}{dt} = C\epsilon^{1/3}L_v^{4/3} \tag{7}$$

In both equations ϵ is the energy dissipation rate and C is a constant equal to 2.14 (Lesieur, 1990). The integral length scale of the velocity fluctuations is a measure for the large-scale turbulent flow structures. Combining Eqs. 5, 6, and 7 yields the following equation for the turbulent dispersion coefficient

$$D_t = 2C\epsilon^{1/3}\lambda^{4/3} \qquad \lambda = L \quad \text{when} \quad L < L_v$$
$$\lambda = L_v \quad \text{when} \quad L > L_v \tag{8}$$

When the momentum of the feedstream is negligible compared to the momentum of the flow in the reactor, the velocity of the feedstream in the reactor will be equal to the local circulation velocity. This is normally the case when the feed velocity is smaller than or comparable to the local circulation velocity (Jeurissen et al., 1994). Under these circumstances, the initial diameter of the dispersed feedstream (L_o) is given

by (Baldyga et al., 1997)

$$Q_f = \frac{\pi}{4} L_o^2 u \tag{9}$$

where Q_f is the feed flow rate and u is the feed velocity just beneath the feed pipe.

To calculate the selectivity of a mixing-sensitive reaction set in a semi-batch stirred tank reactor, a mass balance is made for each component i inside a fluid element added to the reactor

$$\frac{dc_i}{dt} = \frac{1}{V_{mi}} \frac{dV_{mi}}{dt} (\langle c_i \rangle - c_i) + R_i \tag{10}$$

in which c_i is the concentration of component i in the mixed volume, $\langle c_i \rangle$ is the concentration of component i in the bulk, and R_i is the specific reaction rate. The growth of the micromixed volume is calculated with Eq. 3 and depends on the volume of the dispersed feedstream. The volume of the dispersed feedstream is calculated with Eqs. 5 and 9. The concentration in the bulk is assumed to be constant during one circulation time, and the added feed liquid is assumed to be homogeneously mixed after one circulation time (Baldyga and Bourne, 1989a; Phillips et al., 1999). Due to this assumption, the history of all fluid elements added to the reactor during one circulation time will be the same. Therefore, the total feed volume is discretized into fluid elements with a volume (V_0) equal to

$$V_0 = V_{\text{feed}} \frac{t_c}{t_{\text{feed}}} \tag{11}$$

where V_{feed} is the total volume, t_c is the circulation time, and t_{feed} is the feed time. The feed time is defined as the total feed volume divided by the feed flow rate. The circulation time inside a stirred tank reactor is given by

$$t_c = \frac{V_{\text{reactor}}}{r_c Q_p} \tag{12}$$

where V_{reactor} is the volume of the reactor contents, r_c is the circulation ratio, and Q_p is the pumping capacity of the stirrer. The pumping capacity of the stirrer is

$$Q_p = N_q N D_{im}^3 \tag{13}$$

where N_q is the flow number of the stirrer, N is the stirrer speed, and D_{im} is the impeller diameter. The flow number and circulation ratio of a Rushton turbine stirrer are equal to 0.7 and 3, respectively (Schoenmakers, 1998).

Hydrodynamic Parameters

The engulfment rate is a function of the local energy dissipation rate. The turbulent dispersion coefficient depends on the local energy dissipation rate and the local velocity length scale. Therefore, these parameters have to be known for the

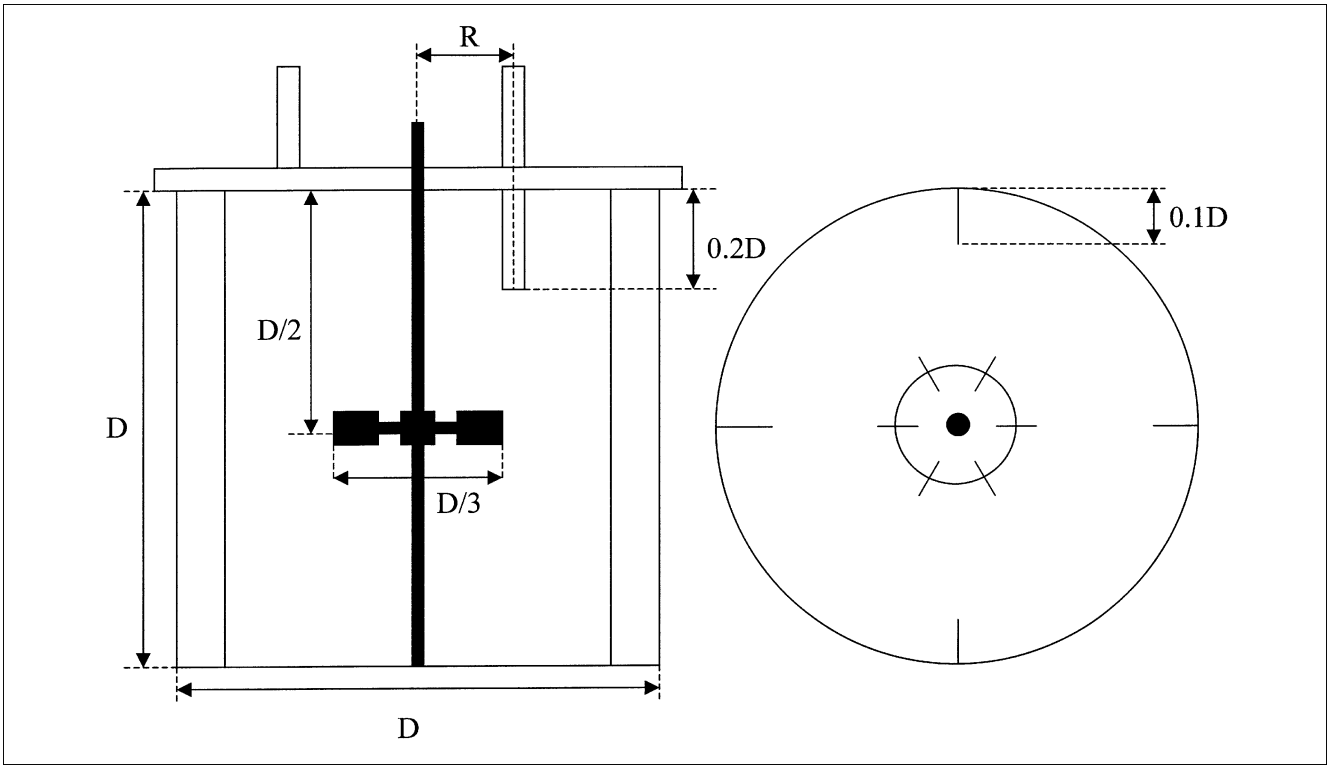

Figure 1. Geometry of the vessels showing a closed top, four baffles, a feed pipe and an effluent pipe.

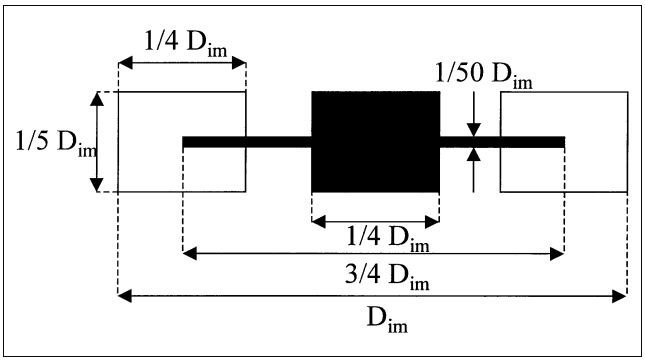

Figure 2. Geometry of the Rushton turbine stirrer.

calculation of the selectivity of a mixing sensitive reaction. A fluid element added to the reactor is followed as it moves through the reactor. When the hydrodynamic parameters vary throughout the vessel, the location of the added fluid element inside the reactor has to be known. This location is determined by the local average velocity inside the stirred vessel. The energy dissipation rate, the velocity length scale, and the local average velocity are dependent on the stirred-tank reactor used. For many industrial processes, these hydrodynamic parameters are not known in detail. In this study, the necessary degree of complexity in the description of these hydrodynamic parameters to obtain a good agreement between the measured and calculated selectivities is investigated.

Energy dissipation rate and velocity length scale

The experimental system used in this study is a cylindrical vessel equipped with a Rushton turbine stirrer, as shown in Figures 1 and 2. The hydrodynamic parameters are determined from the previous laser doppler velocimetry measurements (Kajbic, 1995; Kusters, 1991; Schoenmakers, 1998). The hydrodynamic parameters are described in three flow maps with different levels of complexity. In these flow maps the local energy dissipation rate is related to the average energy dissipation rate

$$\bar{\epsilon} = \frac{N_p N^3 D_{im}^5}{V_{\text{reactor}}} \tag{14}$$

in which N_p is the power number, equal to 5.3 for the stirrer used in this work (Schoenmakers, 1998).

Flow map 1. In the first flow map the hydrodynamic parameters are assumed to be constant throughout the whole vessel. The energy dissipation rate is taken equal to the average energy dissipation rate calculated with Eq. 13. The velocity length scale is taken equal to the baffle width.

Flow map 2. In the second flow map, the vessel is divided into three regions, as illustrated in Figure 3. The energy dissipation rates in these regions are described by correlations given by Schoenmakers et al. (1996)

$$\text{bulk region:} \quad \epsilon = 0.13\bar{\epsilon} \tag{15}$$

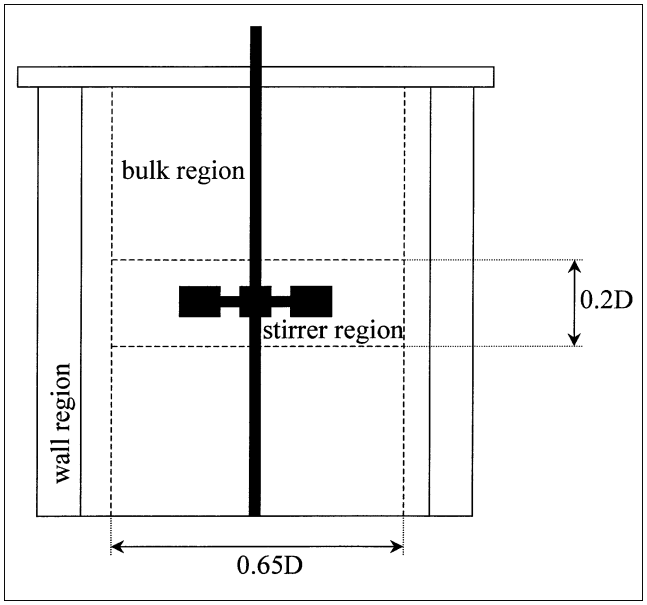

Figure 3. Division of the reactor into three regions having different hydrodynamic parameters.

$$\text{stirrer region:} \quad \epsilon = 7.3\bar{\epsilon} \tag{16}$$

$$\text{wall region:} \quad \epsilon = 0.63\bar{\epsilon} \tag{17}$$

In the bulk region, the velocity length scale equals 0.15 times the vessel diameter (Schoenmakers, 1998). The velocity length scale in the stirrer region is equal to the impeller blade width (Kusters, 1991). Experimental data of the velocity length scale in the wall region are not available. As velocity length scales are related to the dimensions of the elements generating the turbulence, the length scale in the wall region is assumed to be equal to the baffle width.

Flow map 3. The third flow map is equal to flow map 2 except for the energy dissipation rate in the stirrer region. Due to large gradients in the energy dissipation rate in the stirrer region, in the third flow map a more detailed description of the energy dissipation rate in stirrer region is used

$$\epsilon = \left(0.414 - 3.462 \cdot \frac{r}{D_{\text{vessel}}} + 8.233 \cdot \left(\frac{r}{D_{\text{vessel}}}\right)^2\right)^{-1} \cdot \bar{\epsilon} \tag{18}$$

This equation is obtained by fitting a polynomial function through measured energy dissipation rates. These energy dissipation rates have been measured at a height of 1/2 the vessel diameter at nine different radial positions (Kajbic, 1995; Schoenmakers et al., 1996). The measured energy dissipation rates and the fitted polynomial equation are shown in Figure 4.

Location of a fluid element

When the energy dissipation rate and the velocity length scale vary throughout the vessel, the location of a fluid element added to the reactor has to be known during the reaction time. The reaction time is defined as the time necessary

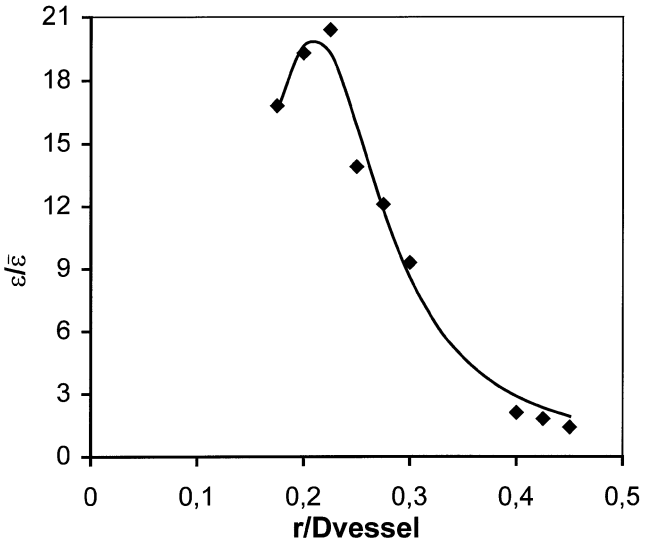

Figure 4. Relative energy dissipation rate profile in the stirrer region.

Points are measured energy dissipation rates with laser doppler velocimetry. The curve is obtained by fitting a polynomial equation through the measured data.

to consume all of the reactants in a fluid element added to the reactor. For the fast chemical reactions considered in this study, this reaction time is always smaller than the circulation time. In the reaction time a fluid element is assumed to flow from the feed pipe through the bulk region towards the stirrer, and then from the stirrer region into the wall region.

The residence time and location of a fluid element in a region is determined by the local average velocity. The residence time in the bulk region is equal to the distance between the feed point and the stirrer region divided by the average velocity over this distance. The average velocity between the feed point and the stirrer region is equal to 0.15 times the stirrer tip speed ($\pi N D_{im}$) (Schoenmakers, 1998).

Inside the stirrer region the average velocity at every radial position (r) is calculated from the pumping capacity of the stirrer

$$v_{\text{stirrer}} = \frac{r_c N_q N D_{im}^3}{0.2 D 2\pi r} \tag{19}$$

A fluid element is assumed to enter the stirrer region at the radial position of the feed pipe (R). With this assumption, the residence time in the stirrer region follows from

$$t_{\text{stirrer}} = \int_R^{0.65D/2} \frac{1}{v_{\text{stirrer}}} dr \tag{20}$$

After a fluid element has left the stirrer region, it is assumed to be in the wall region in the remaining reaction time.

Experimental verification of the model

The model presented earlier is used in combination with the flow maps presented in the previous paragraph to calculate the selectivity of a mixing-sensitive reaction set. The calculated selectivities are validated against experimentally determined selectivities for several process and design variables.

The experiments were performed in geometrically similar vessels of 6 L, 19 L, and 44 L, respectively, equipped with a Rushton turbine stirrer. The geometry of the vessels is shown in Figure 1. The diameters of the vessels were 0.2 m, 0.288 m, and 0.382 m, respectively. The feed pipe diameters for the 6 L, 19 L, and 44 L vessel were 5 mm, 8 mm, and 10 mm, respectively. The radial position of the feed pipe (R) for the 6 L and the 44 L vessels was 0.2 times the vessel diameter, and the radial position of the feed pipe for the 19 L vessel was 0.3 times the vessel diameter. The stirrer Reynolds number (ND_{im}^2/ν) was varied from 6.7 10^3 to 4 10^4 in the 6L vessel and from 1.6 10^4 to 9.7 10^4 in the 44L vessel. In the 19L vessel the stirrer Reynolds number was equal to 1.4 10^4 and 3.7 10^4. The geometry of the Rushton turbine stirrers is shown in Figure 2.

The mixing sensitive reaction set used in this work to validate the mixing model was the third Bourne reaction (Bourne and Yu, 1994). The third Bourne reaction consists of the following two competitive reactions

$$\text{NaOH} + \text{HCl} \xrightarrow{k_1} \text{NaCl} + \text{H}_2\text{O}$$

$$\text{NaOH} + \text{CH}_2\text{ClCOOC}_2\text{H}_5 \xrightarrow{k_2} \text{CH}_2\text{ClCOONa} + \text{C}_2\text{H}_5\text{OH}$$

The second-order kinetic constants for this reaction system are (Baldyga and Bourne, 1999)

$$k_1 = 1.3\ 10^8\ \text{m}^3/(\text{mol s}) \text{ at } 298\ \text{K}$$

$$k_2 = 0.030\ \text{m}^3/(\text{mol s}) \text{ at } 298\ \text{K}$$

For engulfment to be the rate determining step of the micromixing process, the Schmidt number must be smaller than 4,000. To calculate the Schmidt numbers of the reactants, diffusion coefficients have been estimated using Eqs. 3–34 and 3–32 given in Perry and Chilton (1973), valid for electrolytes at infinite dilution and nonelectrolytes at low-concentrations, respectively. The Schmidt numbers of hydrochloric acid, sodium hydroxide and ethyl chloroacetate in water are 300, 470, and 1,200, respectively.

Before each experiment, the vessel was entirely filled with a solution of 0.09 M ethyl chloroacetate (ECA) and 0.09 M HCl. The feedstream was a solution of 1.8 M NaOH and the feed volume was 1/20 of the vessel volume. When the feed was added, solution left the reactor through an effluent pipe positioned at the top of the vessel, as shown in Figure 1.

The reaction between NaOH and HCl is much faster than the reaction between NaOH and ECA. NaOH will only react significantly with ECA when the reaction between NaOH and HCl is limited by mixing. Therefore, the amount of ethanol produced will increase when the mixing rate decreases. The amount of ethanol and ECA present at the end of an experiment in the reactor and in the solution leaving the reactor were determined chromatographically (HPLC). The mixtures

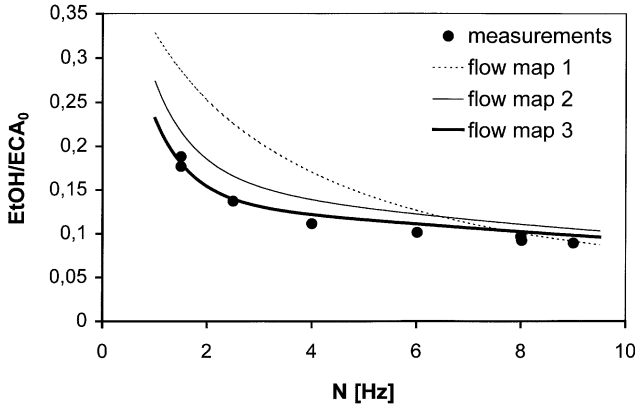

Figure 5. Calculated ethanol yields with the three flow maps and measured ethanol yields vs. stirrer speed for the 6 L vessel and a feed rate equal to the local circulation velocity ($0.15v_{tip}$).

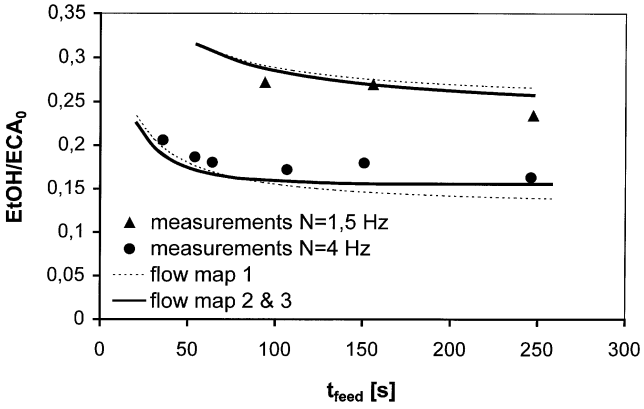

Figure 7. Calculated ethanol yields with the three flow maps and measured ethanol yields as a function of feed time for the 19 L vessel and stirrer speeds of 1.5 Hz and 4 Hz.

were analyzed immediately to avoid the acid catalyzed hydrolysis of ethyl chloroacetate (Baldyga and Bourne, 1999).

As the reaction between NaOH and HCl is almost instantaneous, the following transformation was used to remove the stiffness from the differential equations and to reduce the number of differential equations to be solved (Baldyga and Bourne, 1989b)

$$u = C_{\mathrm{NaOH}} - C_{\mathrm{HCl}} \tag{21}$$

$$C_{\mathrm{NaOH}} = \frac{|u| + u}{2}$$

$$C_{\mathrm{HCl}} = \frac{|u| - u}{2}$$

The mass balances for u and ECA are

$$\frac{du}{dt} = \frac{1}{V_{mi}} \frac{dV_{mi}}{dt} (\langle u \rangle - u) - k_2 C_{\mathrm{ECA}} \left(\frac{|u| + u}{2} \right) \tag{22}$$

$$\frac{dC_{\mathrm{ECA}}}{dt} = \frac{1}{V_{mi}} \frac{dV_{mi}}{dt} (\langle C_{\mathrm{ECA}} \rangle - C_{\mathrm{ECA}}) - k_2 C_{\mathrm{ECA}} \left(\frac{|u| + u}{2} \right) \tag{23}$$

Results and Discussion

The experimentally determined selectivities are compared here with the calculated selectivities. The selectivity is defined as one minus the ethanol yield. The ethanol yield is given as the total amount of ethanol present at the end of an experiment in the reactor and in the solution leaving the reactor divided by the amount of ECA present at the beginning of an experiment.

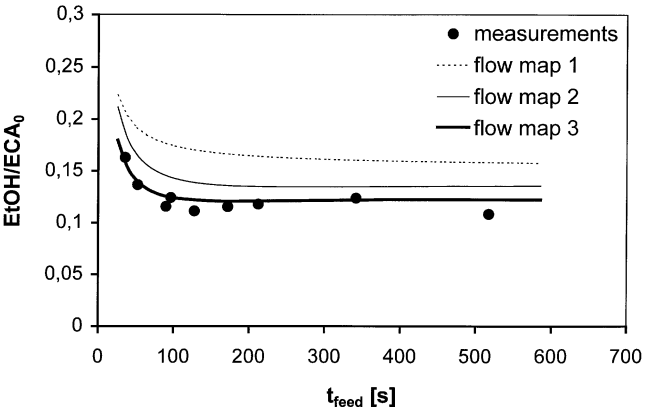

Figure 6. Calculated ethanol yields with the three flow maps and measured ethanol yields as a function of feed time for the 6 L vessel and a stirrer speed of 4 Hz.

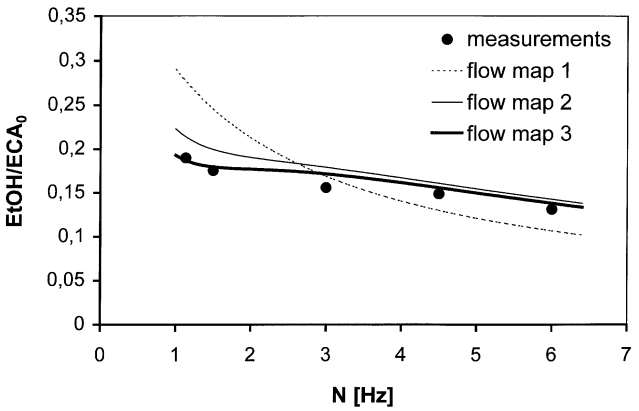

Figure 8. Calculated ethanol yields with the three flow maps and measured ethanol yields vs. stirrer speed for the 44 L vessel and a feed rate equal to the local circulation velocity.

In Figures 5 and 6 measured and calculated ethanol yields for the 6 L vessel are given as a function of stirrer speed and feed time, respectively. Figure 7 shows a comparison between the measured and calculated ethanol yields vs. feed time for the 19 L vessel and two stirrer speeds. In Figure 8 measured and calculated ethanol yields vs. stirrer speed are given for the 44 L vessel. From Figures 5 to 8, it is concluded that an agreement between the measurements and simulations could not be obtained when using constant hydrodynamic parameters. However, good agreement between the measured and calculated selectivities is obtained when a flow map with three characteristic regions is used. Figures 5, 7, and 8 show an increasing selectivity with increasing stirrer speed. Figures 6 and 8 show that, for short feed times, the selectivity decreases with decreasing feed time. This is in agreement with a mixing rate that becomes more controlled by the turbulent dispersion process when the feed time is reduced. For the longer feed times, the selectivity is independent of feed time.

From Figures 5 to 8, it is concluded that the necessary detailing in the description of the hydrodynamic parameters depends on the feed position. The radial feed location was 0.2 times the vessel diameter for the 6 L and 44 L vessel and 0.3 times the vessel diameter for the 19 L vessel. For the 6 L and 44 L vessel, a good agreement between the measured and calculated ethanol yields is observed when flow map 3 is used. For the 19 L vessel, already a reasonable agreement between the measured and calculated ethanol yields is observed when constant hydrodynamic parameters are used. A good agreement between the measured and calculated ethanol yields is obtained for the 19 L vessel when flow map 2 is used. The calculated ethanol yields with flow map 2 and 3 coincide in Figure 7. The influence of the feed position on the necessary degree of complexity in the description of the hydrodynamic parameters will be discussed in more detail below.

In Figures 9 and 10 the growth of the micromixed volume in the feedstream, calculated with the three different flow maps, is plotted vs. the dimensionless time (t/t_c) for the 6 L and 19 L vessel, respectively. On the lower horizontal axis of these figures, the residence times of a fluid element in the bulk region and in the stirrer region are given. A fluid element is assumed to enter the stirrer region at the radial position of the feed pipe. Therefore, the residence time in the stirrer region for the 19 L vessel is shorter than for the 6 L vessel. In Figure 9 a large deviation between the micromixed volumes in the stirrer region calculated with flow maps 1 and 3 is observed for the 6 L vessel. For the 19 L vessel, the residence time in the stirrer region is too short to result in a large difference between these micromixed volumes. For both vessels, large deviations between the micromixed volumes calculated with flow map 1 and flow map 3 are observed in the bulk region. However, in the bulk region the growth of the micromixed volume is small; therefore, only a small amount of ethanol will be produced in this region. Apparently, the residence time in the stirrer region of the 19 L vessel is too short and the amount of ethanol produced in the bulk region is too small to generate a large difference between the calculated ethanol yields with flow map 1 and flow map 3, respectively.

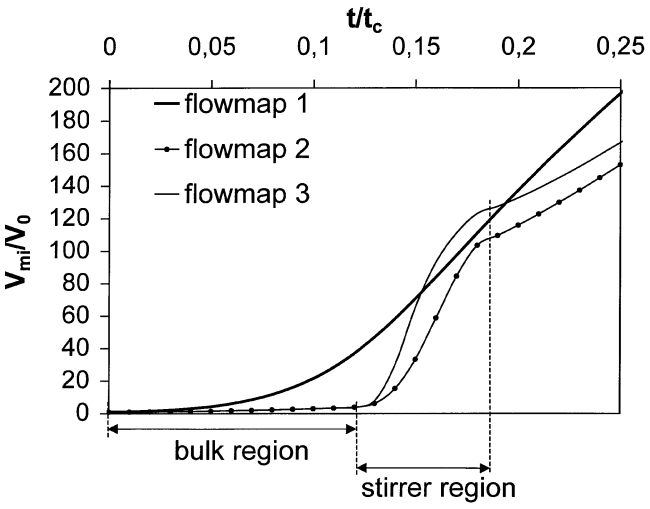

Figure 9. MIcromixed volume as a function of dimensionless time (t/t_c) for the 6 L vessel, a stirrer speed of 4 Hz and a feed time of 127 s.

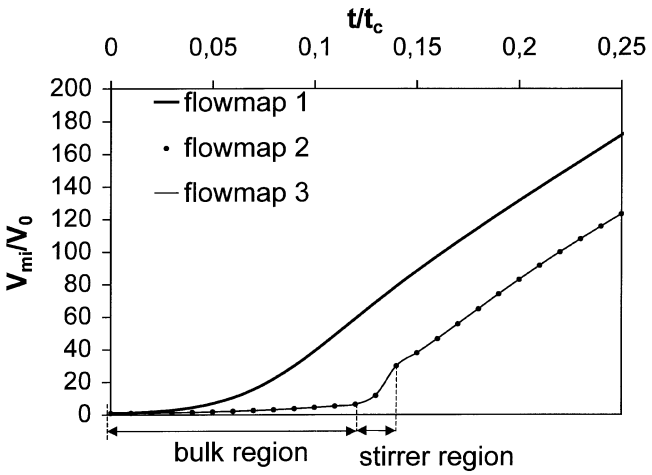

Figure 10. Micromixed volume as a function of dimensionless time (t/t_c) for the 19 L vessel, a stirrer speed of 4 Hz, and feed time of 103 s.

For the 6 L and 44 L vessel, the energy dissipation rate in the stirrer region described by flow map 3 is higher than the average energy dissipation rate in the stirrer region of flow map 2. Consequently, in Figures 5, 6, and 8 the calculated ethanol yields with flow map 3 are lower than the calculated ethanol yields with flow map 2. For the 19 L vessel, the energy dissipation rate in the stirrer region described by flow map 3 is almost equal to the average energy dissipation rate in the stirrer region used in flow map 2. Therefore, the ethanol yields calculated with flow map 2 and flow map 3 coincide in Figure 7.

In Figure 11 the dimensionless volume of the dispersed feedstream (V_{td}/V_0) and the dimensionless micromixed volume (V_{mi}/V_0) are given as a function of the dimensionless time (t/t_c) for several stirrer speeds. These volumes are calculated with flow map 3 with the same process parameters as used to calculate the selectivity in Figure 5. The volume of the dispersed feedstream as a function of the dimensionless time is the same for all stirrer speeds, because $V_{td} \sim N$ and

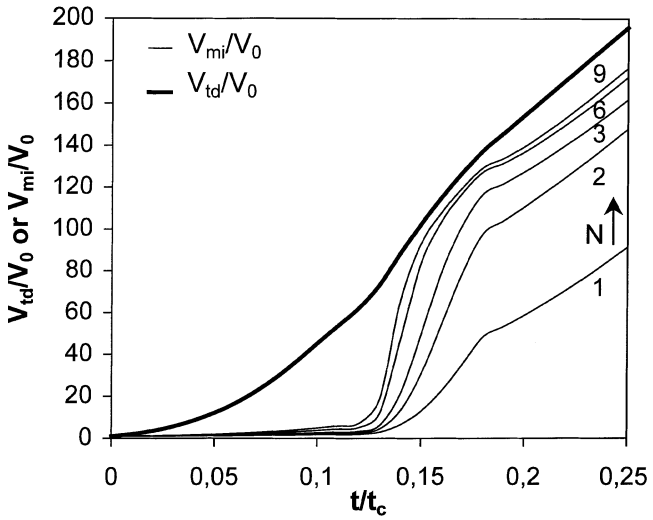

Figure 11. Volume of the dispersed feed stream (V_{td}) and the micromixed volume (V_{mi}) as a function of dimensionless time (t/t_c) and stirrer speed for the 6 L vessel, and a feed rate equal to the local circulation velocity ($0.15v_{tip}$).

$t_c \sim N^{-1}$. The micromixed volume as a function of the dimensionless time increases with increasing stirrer speed. Therefore, the volume fraction of micromixed fluid inside the dispersed feedstream increases when the stirrer speed is increased, resulting in more self-engulfment and, consequently, a smaller increase in the growth rate of the micromixed volume for the higher stirrer speeds. For stirrer speeds above 3 Hz, the increase in the growth rate of the micromixed volume with increasing stirrer speed is relatively small. This effect can also be observed in Figure 5 by a decreasing influence of the stirrer speed on the selectivity for stirrer speeds higher than 3 Hz.

Conclusions

In this article a model is proposed for the prediction of the product quality of fast chemical reactions in semi-batch stirred-tank reactors. Application of this model requires information on the energy dissipation rate, the velocity length scale, and the average velocity. The local values for these parameters vary throughout the stirred tank and, therefore, the agreement between measured and calculated selectivities depends on the complexity of the flow map describing these hydrodynamic parameters. When these hydrodynamic parameters are described in sufficient detail, the proposed mixing model is able to predict the selectivity of a mixing-sensitive reaction. This will allow for the effective design and scale-up of stirred-tank reactors in which this type of reaction is carried out.

The model presented in this article has been validated by determining the product distribution of the third Bourne reaction. During the experiments, the feed velocity was smaller than or comparable to the local circulation velocity. Therefore, the influence of the feedstream on the hydrodynamic parameters has been neglected. Under these circumstances, an agreement between the measured and calculated product distributions could not be obtained when using constant hydrodynamic parameters in the entire vessel. However, a flow map with three characteristic region is sufficient to obtain a good agreement between the measurements and the simulations. In this flow map, the velocity length scale is constant in each region and the energy dissipation rate has a constant value in the bulk region and in the wall region. Since large gradients in the energy dissipation rate are present in the stirrer region, the necessary detailing in the description of the energy dissipation rate depends on the radial position of the feed pipe. When the radial position of the feed pipe is equal to 0.3 times the vessel diameter, a constant energy dissipation rate in the stirrer region can be used. However, when the radial position of the feed pipe is equal to 0.2 times the vessel diameter, a description of the gradient in the energy dissipation rate in the stirrer region is necessary.

Notation

c_i = concentration of component i in the mixed volume, $\text{mol}\cdot\text{m}^{-3}$
$\langle c_i \rangle$ = concentration of compound i in the bulk, $\text{mol}\cdot\text{m}^{-3}$
D_{im} = impeller diameter, m
D_t = turbulent dispersion coefficient, $\text{m}^2\cdot\text{s}^{-1}$
D_{vessel} = vessel diameter, m
E = engulfment rate, s^{-1}
k_i = kinetic constant, $\text{m}^3\cdot\text{mol}^{-2}\cdot\text{s}^{-1}$
L = linear dimension of a scalar cloud, m
L_o = initial diameter of the dispersed feedstream, m
L_v = length scale of the velocity fluctuations, m
N = stirrer speed, s^{-1}
N_p = power number
N_q = stirrer flow number
Q_p = stirrer pumping capacity, $\text{m}^3\cdot\text{s}^{-1}$
r = radial coordinate, m
r_c = circulation ratio
R_i = reaction rate, $\text{mol}\cdot\text{m}^{-3}\cdot\text{s}^{-1}$
t = time, s
t_c = circulation time, s
t_{feed} = feed time, s
t_{stirrer} = residence time in the stirrer region, s
u = velocity, $\text{m}\cdot\text{s}^{-1}$
v_{stirrer} = velocity in the stirrer region, $\text{m}\cdot\text{s}^{-1}$
V_o = volume of a fluid element, m^3
V_{feed} = feed volume, m^3
V_{mi} = volume mixed on a molecular, scale m^3
V_{reactor} = volume of the reactor contents, m^3
V_{td} = volume of the dispersed feed stream, m^3
δ = thickness, m
ϵ = energy dissipation rate, $\text{m}^2\cdot\text{s}^{-3}$
ν = kinematic viscosity, $\text{m}^2\cdot\text{s}^{-1}$

Acknowledgments

We would like to thank the undergraduate students Bjorn Hultermans and Martijn Reubzaet for their contribution in this work.

Literature Cited

Baldyga, J., and J. R. Bourne, "A Fluid Mechanical Approach to Turbulent Mixing Part II Micromixing in the Light of Turbulence Theory," *Chem. Eng. Commun.*, **28**, 243 (1984).

Baldyga, J., and J. R. Bourne, "Simplification of Micromixing Calculations I. Derivation and Application of New Model," *Chem. Eng. J.*, **42**, 83 (1989a).

Baldyga, J., and J. R. Bourne, "Simplification of Micromixing Calculations II. New Applications," *Chem. Eng. J.*, **42**, 93 (1989b).

Baldyga, J., and J. R. Bourne, "Interactions Between Mixing on Various Scales in Stirred Tank Reactors," *Chem. Eng. Sci.*, **47**, 1839 (1992).
Baldyga, J., and J. R. Bourne, *Turbulent Mixing and Chemical Reactions*, Wiley, Chichester, U.K. (1999).
Baldyga, J., J. R. Bourne, and S. J. Hearn, "Interaction Between Chemical Reactions and Mixing on Various Scales," *Chem. Eng. Sci.*, **52**, 457 (1997).
Baldyga, J., and R. Pohorecki, "Turbulent Micromixing in Chemical Reactors—a Review," *Chem. Eng. J.*, **58**, 183 (1995).
Bourne, J. R., and P. Dell'ava, "Micro- and Macro-Mixing in Stirred Tank Reactors of Different Sizes," *Chem. Eng. Res. Des.*, **65**, 180 (1987).
Bourne, J. R., and S. Yu, "Investigation of Micromixing in Stirred Tank Reactors Using Parallel Reactions," *Ind. Eng. Chem. Res.*, **33**, 41 (1994).
David, R., and J. Villermaux, "Interpretation of Micromixing Effects on Fast Consecutive-Competing Reactions in Semi-Batch Stirred Tanks by a Simple Interaction Model," *Chem. Eng. Commun.*, **54**, 333 (1987).
Franke, J., and A. Mersmann, "The Influence of the Operation Conditions on the Precipitation Process," *Chem. Eng. Sci.*, **50**, 1737 (1995).
Fox, R. O., "Computational Methods for Turbulent Reacting Flows in the Chemical Process Industry," *Revue de L'institut Français du Pétrole*, **51**, 215 (1996).
Jacobson, A. R., A. N. Makris, and L. M. Sayre, "Monoacylation of Symmetrical Diamines," *J. Org. Chem.*, **52**, 2592 (1987).
Jeurissen, F., J. G. Wijers, and D. Thoenes, "Initial Mixing of Feed Streams in Agitated Vessels," *I. Chem. E. Symp. Series*, **136**, 235 (1994).
Kajbic, A. F., *Distribution of Energy Dissipation in Stirred Vessels for Liquids and Suspensions*, (in Dutch), Eindhoven University of Technology, Institute for Continuing Education, (1995).
Kusters, K. A., "The Influence of Turbulence on Aggregation of Small Particles in Agitated Vessels," PhD Thesis, Eindhoven University of Technology (1991).
Larsson, G., S. George, and S. O. Enfors, Scale-Down Reactor Model to Simulate Insufficient Mixing Conditions During Fed Batch Operation Using a Biological Test System," *Process Mixing-Chemical and Biochemical Applications, AIChE Symp. Series*, **293**, 151 (1992).
Lesieur, M., *Turbulence in Fluids: Stochastic and Numerical Modeling*, Kluwer Academic Publishers, Dordrecht, The Netherlands (1990).
Nagata, S., *Mixing*, Wiley, New York (1975).
Perry, R. H., and C. H. Chilton, *Chemical Engineers' Handbook*, Fifth ed., McGraw-Hill, New York (1973).
Phillips, R., S. Rohani, and J. Baldyga, "Micromixing in a Single Feed Semi-Batch Precipitation Process," AIChE J., **45**, 82 (1999).
Ranade, V. V., and J. R. Bourne, "Reactive Mixing in Agitated Tanks," *Chem. Eng. Commun.*, **99**, 33 (1991).
Schoenmakers, J. H. A., "Turbulent Feed Stream Mixing in Agitated Vessels," PhD Thesis, Eindhoven University of Technology (1998).
Schoenmakers, J. H. A., J. G. Wijers, and D. Thoenes, "Simplified Stirrer Modeling for the Prediction of Time Averaged Hydrodynamics in Stirred Vessels," *Proc. Fluid Mixing 5 Conf.*, 327 (1996).
Manuscript received Aug. 7, 2000, and revision received Dec. 21, 2000.